

# Dynamical light vector mesons in low-energy scattering of Goldstone bosons

I.V. Danilkin,<sup>a,b</sup> L.I.R. Gil,<sup>a</sup> and M.F.M. Lutz<sup>a</sup>

<sup>a</sup>*GSI Helmholtzzentrum für Schwerionenforschung GmbH,  
Planck Str. 1, 64291 Darmstadt, Germany*

<sup>b</sup>*Institute for Theoretical and Experimental Physics,  
117259, B. Cheremushkinskaya 25, Moscow, Russia*

---

## Abstract

We present a study of Goldstone boson scattering based on the flavor SU(3) chiral Lagrangian formulated with vector mesons in the tensor field representation. A coupled-channel computation is confronted with the empirical s- and p-wave phase shifts, where good agreement with the data set is obtained up to about 1.2 GeV. There are two relevant free parameters only, the chiral limit value of the pion decay constant and the coupling constant characterizing the decay of the rho meson into a pair of pions. We apply a recently suggested approach that implements constraints from micro-causality and coupled-channel unitarity. Generalized potentials are obtained from the chiral Lagrangian and are expanded in terms of suitably constructed conformal variables. The partial-wave scattering amplitudes are defined as solutions of non-linear integral equations that are solved by means of an N/D ansatz.

---

## 1 Introduction

The study of Goldstone boson interactions is a time honored challenge in hadron physics [1,2,3,4,5,6,7,8]. In the last decade there was significant progress in a profound description and understanding of the low-energy regime based on the chiral Lagrangian. In the close-to-threshold region chiral perturbation theory ( $\chi$ PT) is applicable and leads to controlled results that are consistent with the empirical scattering data [9,10,11,12,13]. Extensions of  $\chi$ PT, that implement coupled-channel unitarity by means of partial summation techniques, aim at a description of the scattering data at somewhat larger energies where meson resonances play an important role [14,15,16,17]. Most remarkable is the systematic computation at the one-loop level where the inverse of the partial-wave amplitudes is expanded in chiral powers [17]. Accurate results for the s- and p-wave phase shifts up to about  $\sqrt{s} \simeq 1.2$  GeV were obtained by adjusting

the  $Q^4$  counter terms of the chiral Lagrangian. This implies that the lowest scalar and vector mesons with  $J^P = 0^+$  and  $1^-$  are properly described by such an approach. It has been argued by detailed large- $N_c$  scaling studies that the nature of the light scalar and vector mesons is distinct [18]. While the scalar mesons may be generated by the leading order terms of the chiral Lagrangian, the vector mesons are a consequence of the subleading counter terms.

The purpose of this Letter is to further explore the dynamic role of light vector mesons in a chiral Lagrangian. The motivation of considering the light vector mesons as explicit degrees of freedom is twofold. First, we recall that it was shown previously that the size of the symmetry preserving  $Q^4$  counter terms may be estimated by a resonance saturation mechanism where the light vector mesons appear to dominate [19]. Second, the light vector mesons play a particular role in the hadrogenesis conjecture [18,20]. Together with the Goldstone bosons, they are identified to be the relevant degrees of freedom that are expected to generate the meson spectrum. For instance it was shown that the leading chiral interaction of Goldstone bosons with the light vector mesons generates an axial-vector meson spectrum that is quite close to the empirical one [20]. From this point of view the axial-vector mesons are similar in nature as the scalar mesons. We consider a chiral Lagrangian with explicit vector meson fields as a promising starting point to compute the meson spectrum.

While it is straightforward to write down a chiral Lagrangian with explicit vector mesons it is an open issue how to order the various terms according to some counting scheme. In a recent work a counting scheme was suggested based on large- $N_c$  arguments and the dynamical assumption of hadrogenesis [18]. So far it has been tested successfully against two and three body decays systematically at the tree level [18,21]. In this work we scrutinize its implication in the scattering of Goldstone bosons. At leading order the vector meson exchange processes should be considered already, rather than at a subleading order, as is implicit in the standard  $\chi$ PT approach. Based on this assumption we perform a coupled-channel computation, where we apply a novel unitarization scheme developed by one of the authors recently [22,23].

Though the inverse amplitude method applied with great success in previous works obtains an inverse amplitude that can be represented in terms of dispersion-integral representation there is a subtle limitation of this approach, if applied to a coupled-channel situation. In the inverse amplitude method or any algebraic approach the partial-wave scattering amplitudes have unphysical left-hand branch points. This holds at any finite truncation. The source of these is easily understood. The locations of the left-hand branch points of a partial-wave scattering amplitude depend decisively on the channel. There is no universal branch point that characterizes all coupled-channel amplitudes. In any algebraic method there is a determinant of functions with left-hand branch points at different locations. Via the determinant a branch point of a

given channel is transported into any other channel as long as the transition potential is non-vanishing. In general this leads to the presence of all possible left-hand branch cuts in all channels. Though this is unphysical it does not necessarily always lead to numerically significant effects in the physical region. If all considered branch points are below the smallest considered threshold typically the presence of unphysical branch points are not really problematic. However, once a left-hand branch point of a heavy channel is located right to the threshold of a lighter channel the limitations of an algebraic approach start to be visible.

The main objective of the novel scheme [22,23] to be applied in this work is a controlled realization of the causality and unitarity condition in a perturbative application of the chiral Lagrangian. The starting points are partial-wave dispersion relations. A generalized potential is constructed from the chiral Lagrangian in the subthreshold region and analytically extrapolated to higher energies. The partial-wave scattering amplitudes are obtained as solutions of non-linear integral equations.

In our scheme the empirical s- and p-wave phase shifts are recovered up to about 1.2 GeV. There are two relevant free parameters only, the chiral limit value of the pion decay constant and the coupling constant characterizing the decay of the rho meson into a pair of pions.

## 2 Chiral Lagrangian with vector meson fields

We recall the leading order chiral Lagrangian for the Goldstone bosons and vector mesons. The vector mesons are represented in terms of anti-symmetric fields  $V_{\mu\nu} = -V_{\nu\mu}$ . It has been demonstrated first in [19], that vector mesons interpolated in terms of anti-symmetric fields provide a transparent saturation model for the  $Q^4$  counter terms of the chiral Lagrangian in its Goldstone boson sector. The chiral Lagrangian is composed out of the building blocks,  $U_\mu$ ,  $V_{\mu\nu}$ ,  $\chi_\pm$ , that transform identically under chiral rotations (see e.g. [24]). We do not consider electromagnetic interactions here. Using covariant derivatives,  $D_\mu$ , the transparent transformation properties are maintained for terms involving derivatives,

$$\begin{aligned} D_\mu V_{\alpha\beta} &= \partial_\mu V_{\alpha\beta} + [\Gamma_\mu, V_{\alpha\beta}]_- , & \Gamma_\mu &= \frac{1}{2} \left( u^\dagger \partial_\mu u + u \partial_\mu u^\dagger \right) , \\ U_\mu &= \frac{1}{2} u^\dagger \left( \partial_\mu e^{i \frac{\Phi}{f}} \right) u , & u &= \exp \left( \frac{i \Phi}{2f} \right) , & \chi_\pm &= \frac{1}{2} u \chi_0 u \pm \frac{1}{2} u^\dagger \chi_0 u^\dagger , \end{aligned} \tag{1}$$

$$\chi_0 = 2 B_0 \begin{pmatrix} m_u & 0 & 0 \\ 0 & m_d & 0 \\ 0 & 0 & m_s \end{pmatrix} = \begin{pmatrix} m_\pi^2 & 0 & 0 \\ 0 & m_\pi^2 & 0 \\ 0 & 0 & 2m_K^2 - m_\pi^2 \end{pmatrix}, \quad (2)$$

where the pseudo-scalar meson octet field  $\Phi$  is normalized as in [18]. There are two types of terms which one has to consider. The ones that break the chiral  $SU(3)$  symmetry explicitly involve the field combinations  $\chi_\pm$  and are proportional to the quark-mass matrix of QCD. At leading order the diagonal matrix  $\chi_0$  can be expressed in terms of the pion and kaon masses as indicated in (2). Isospin breaking effects are neglected. We consider further constraints from QCD as they arise in the limit of a large number of colors  $N_c$  [18]. This implies that interaction terms that involve a double trace in flavor space can be neglected. The latter are suppressed by  $1/N_c$  as compared to single-flavor trace interactions. To order  $Q^2$  the following terms were proposed in [18] to be relevant in our case

$$\begin{aligned} \mathcal{L} = & f^2 \text{tr} \left\{ U^\mu U_\mu^\dagger + \frac{1}{2} \chi_+ \right\} - \frac{1}{4} \text{tr} \left\{ (D^\mu V_{\mu\alpha}) (D_\nu V^{\nu\alpha}) \right\} \\ & + \frac{1}{8} m_{1-}^2 \text{tr} \left\{ V^{\mu\nu} V_{\mu\nu} \right\} + \frac{1}{8} b_D \text{tr} \left\{ V^{\mu\nu} V_{\mu\nu} \chi_+ \right\} + i \frac{m_V h_P}{2} \text{tr} \left\{ U_\mu V^{\mu\nu} U_\nu \right\} \end{aligned} \quad (3)$$

where  $f \simeq f_\pi$  may be identified with the pion-decay constant,  $f_\pi = 92.4$  MeV, at leading order. A precise determination of  $f$  requires a chiral  $SU(3)$  extrapolation of some data set. In [25] the value  $f \simeq 90$  MeV obtained from a detailed study of pion- and kaon-nucleon scattering data. This value was used consistently in various applications of chiral Lagrangians to meson and baryon resonance physics [26,27,28]. We discriminate the mass of the light vector mesons  $m_{1-}$  and the scale parameter  $m_V$ . From [18,21] we recall the value for the parameter,  $h_P$ , as determined by two and three-body decay properties of the light vector mesons

$$h_P = 0.29 \pm 0.03 \quad \text{for} \quad m_V = 776 \text{ MeV} \quad (4)$$

at tree-level computations. A first coupled-channel computation based on (3), was presented in [20] where the scattering of Goldstone bosons off the vector mesons was considered. The axial-vector meson spectrum was generated dynamically.

### 3 Coupled-channel dynamics

Given the Lagrangian (3) we compute the two-body coupled-channel scattering amplitudes. At tree-level the scattering amplitude takes the generic form

$$\begin{aligned}
T(s, t, u) = & \frac{C_s}{12f^2} s + \frac{C_t}{12f^2} t + \frac{C_u}{12f^2} u + \frac{C_\pi}{12f^2} m_\pi^2 + \frac{C_K}{12f^2} m_K^2 \\
& + \sum_{x=0}^8 \frac{(m_V h_P)^2}{128f^4} \frac{C_{s-ch}^{(x)}}{s - m_x^2} \left[ (s + m_2^2 - m_1^2)(s + \bar{m}_2^2 - \bar{m}_1^2) + 2(t - m_2^2 - \bar{m}_2^2)s \right] \\
& + \sum_{x=0}^8 \frac{(m_V h_P)^2}{128f^4} \frac{C_{t-ch}^{(x)}}{t - m_x^2} \left[ (t + m_2^2 - \bar{m}_2^2)(t + m_1^2 - \bar{m}_1^2) + 2(s - m_2^2 - m_1^2)t \right] \\
& + \sum_{x=0}^8 \frac{(m_V h_P)^2}{128f^4} \frac{C_{u-ch}^{(x)}}{u - m_x^2} \left[ (u + m_2^2 - \bar{m}_1^2)(u + \bar{m}_2^2 - m_1^2) + 2(t - m_2^2 - \bar{m}_2^2)u \right],
\end{aligned} \tag{5}$$

where the coefficients  $C_{\dots}$  depend on the channel, in particular on isospin ( $I$ ) and strangeness ( $S$ ). We refrain from detailing the various coefficients since they can easily be calculated and mostly have been given previously [17]. The sums in (5) extend over the members of the vector meson nonet, where  $m_x$  denotes their respective masses. The sum of the Mandelstam variables  $s + t + u = m_1^2 + m_2^2 + \bar{m}_1^2 + \bar{m}_2^2$  is the sum of the squared meson masses, where we use a bar for the final state masses. Partial-wave amplitudes are introduced by an average

$$T^J(s) = \int_{-1}^{+1} \frac{d \cos \theta}{2} \left( \frac{s}{\bar{p}_{\text{cm}} p_{\text{cm}}} \right)^J T(s, t, u) P_J(\cos \theta), \tag{6}$$

over the center-of-mass scattering angle  $\theta$ . The relative momenta of the initial and final state are denoted by  $p_{\text{cm}}$  and  $\bar{p}_{\text{cm}}$ . The total angular momentum is  $J$ .

The coupled-channel partial-wave amplitudes  $T_{ab}^J(s)$  are determined as solutions of the non-linear integral equation

$$T_{ab}^J(s) = U_{ab}^J(s) + \sum_{c,d} \int_{\mu_{thr}^2}^{\infty} \frac{d\bar{s}}{\pi} \frac{s - \mu_M^2}{\bar{s} - \mu_M^2} \frac{T_{ac}^J(\bar{s}) \rho_{cd}^J(\bar{s}) T_{db}^{J*}(\bar{s})}{\bar{s} - s - i\epsilon}, \tag{7}$$

with the phase-space matrix

$$\rho_{ab}^J(s) = \frac{1}{8\pi} \left( \frac{p_{cm}}{\sqrt{s}} \right)^{2J+1} \delta_{ab}. \tag{8}$$

The matching scale  $\mu_M^2$  is identified with the smallest two-body threshold accessible in a sector with isospin and strangeness ( $I, S$ ).

Given a generalized potential  $U_{ab}^J(s)$  the non-linear integral equation implies a partial-wave scattering amplitude  $T_{ab}^J(s)$  that complies with the coupled-channel unitarity request and the microcausality condition. On the other hand

the crossing symmetry constraint is not automatically satisfied [29]. If crossing symmetry would be implemented exactly, a crossed reaction can be computed from the direct reaction amplitude. Necessarily, the crossed reaction would be determined by the direct reaction amplitude evaluated at energies below the  $s$ -channel threshold. Now, imagine that in a first step we have some means to approximate the generalized potential systematically and very accurately at energies above the  $s$ -channel threshold only. We may use this potential and determine via (7) the scattering amplitude in the physical region. In this case we are not able to compute the crossed reaction, since our approximation for the generalized potential is valid above threshold only, by assumption. The crossed reaction may be computed by setting up the analogous non-linear integral equation (7) for the crossed reaction. It involves potentials distinct from the potentials of the direct reaction. But where is the crossing symmetry constraint? Our argument illustrates that crossing symmetry is a constraint that affects dominantly amplitudes at subthreshold energies. In a second step we now imagine that we have some means to approximate the generalized potential systematically at energies  $\sqrt{s} \geq \Lambda_0$ , i.e. we include a small subthreshold region. In this case crossing symmetry does provide a constraint. The crossed reaction amplitude can be computed from the direct amplitudes, however, only in a specific subthreshold region. The coincidence of the crossing transformed amplitudes and the amplitudes from the crossed reaction in that specific subthreshold region defines the desired constraint. Note that a non-empty coincidence region requires  $\Lambda_0$  to be sufficiently distinct from the  $s$ -channel unitarity branch point. In our scheme a measure for the amount of crossing-symmetry violation is the strength of non-perturbative contributions to the subthreshold scattering amplitudes.

The non-linear integral equation (7) does not necessarily have a solution or it can have several. A unique solution is singled out by the condition that in a small vicinity of the matching point  $\mu_M^2$ , the results of chiral perturbation theory are recovered. This implies a significant suppression of possible crossing-symmetry violating contributions. From the form of (7) it follows that the existence of a solution requires the generalized potential to be bounded asymptotically, modulo some possibly logarithm terms. Thus, an evaluation of  $U_{ab}^J(s)$  in  $\chi$ PT is futile. Any finite order truncation leads to unbounded potentials, characterized by an asymptotic growth in some power of  $s$ . However, as was pointed out in [22,23], the generalized potential  $U_{ab}^J(s)$  can be reconstructed unambiguously in terms of its derivatives at a point  $\mu_{ab,E}^2$  that lies within its analyticity domain and where the results of  $\chi$ PT are reliable. A solution of (7) requires the knowledge of the generalized potential,  $U_{ab}^J(s)$ , for real energies larger than the maximum of the initial and final thresholds only. Following [22] we identify  $\mu_E$  with the mean of initial and final thresholds. A Taylor expansion of  $U(s)$  around  $\mu_E^2$  has a small convergence radius, that is determined by the distance to the closest left-hand cut. In our case the closest left-hand cuts reflect the two-body  $t$ - and  $u$ -channel unitarity condition.

In order to extend the convergence up to some cutoff scale  $\Lambda_s$ , we apply the conformal map, that was constructed in [22]. Explicitly, it is given by

$$\xi(s) = \frac{a(\Lambda_s^2 - s)^2 - 1}{(a - 2b)(\Lambda_s^2 - s)^2 + 1}, \quad a = \frac{1}{(\Lambda_s^2 - \mu_E^2)^2}, \quad b = \frac{1}{(\Lambda_s^2 - \Lambda_0^2)^2}, \quad (9)$$

where the parameter  $\Lambda_0$  is identified unambiguously such that the mapping domain of the conformal map touches the closest left-hand branch point. Within this domain the generalized potential can be reconstructed in terms of its derivative at the expansion point  $\mu_E^2$ . It holds

$$U(s) = \sum_{k=0}^{\infty} c_k \xi^k(s) \quad \text{for } s < \Lambda_s^2, \quad (10)$$

where the coefficient  $c_k$  is determined by the first  $k$  derivatives of  $U(s)$  at  $\mu_E^2$ . In our analysis the coefficient  $c_k$  are all determined from (5) by the masses of the pseudo-scalar and vector mesons and the two parameters  $f$  and  $h_P$ . It is emphasized that given our construction any contribution, be it a tree-level or loop term, contributes to the generalized potential exclusively via its derivatives at the expansion point. All left-hand cut structures are 'integrated' out systematically. In this work we construct the generalized potential  $U_{ab}^J(s)$  in terms of its first few derivatives at the expansion point  $\mu_E^2$ , where we use the derivatives implied by the tree-level amplitude (5). Via (10) we obtain an approximate generalized potential for energies  $\Lambda_0 < \sqrt{s} < \Lambda_s$ . For energies larger than the cutoff scale  $\Lambda_s$  the generalized potentials are set to a constant [22]. By virtue of the specific form of the conformal map this is a smooth procedure.

It remains to find the desired solution of (7). This is readily achieved in application of the  $N/D$  technique [30]. The partial-wave scattering amplitude is decomposed as

$$T_{ab}(s) = \sum_c D_{ac}^{-1}(s) N_{cb}(s). \quad (11)$$

Again, contributions of right- and left-hand cuts are separated.  $D_{ab}(s)$  contains only the right-hand s-channel unitarity cuts. With the ansatz

$$D_{ab}(s) = \delta_{ab} - \frac{s - \mu_M^2}{s - M_{CDD}^2} R_{ab}^{(D)} - \sum_c \int_{\mu_{thr}^2}^{\infty} \frac{d\bar{s}}{\pi} \frac{s - \mu_M^2}{\bar{s} - \mu_M^2} \frac{N_{ac}(\bar{s}) \rho_{cb}(\bar{s})}{\bar{s} - s}, \quad (12)$$

the coupled-channel unitarity is ensured [22]. In (12) we allow for one CDD pole structure [31] with its pole mass parameter  $M_{CDD}$  and coupling matrix

$R^{(D)}$ . Such a term is requested by the presence of the s-channel vector meson exchange process in some  $J = 1$  amplitudes [32,33]. The matrix  $N_{ab}(s)$  contains left-hand cuts only. If the ansatz (11) is to represent a solution of the non-linear equation (7) the matrix function  $N_{ab}(s)$  has to satisfy the linear integral equation

$$N_{ab}(s) = U_{ab}^{\text{eff}}(s) - \frac{s - \mu_M^2}{s - M_{CDD}^2} \left[ R_{ab}^{(B)} + \sum_c R_{ac}^{(D)} U_{cb}^{\text{eff}}(s) \right] + \sum_{c,d} \int_{\mu_{\text{thr}}^2}^{\infty} \frac{d\bar{s}}{\pi} \frac{s - \mu_M^2}{\bar{s} - \mu_M^2} \frac{N_{ac}(\bar{s}) \rho_{cd}(\bar{s}) [U_{db}^{\text{eff}}(\bar{s}) - U_{db}^{\text{eff}}(s)]}{\bar{s} - s}, \quad (13)$$

with

$$\begin{aligned} U_{ab}^{\text{eff}}(s) &= U_{ab}(s) + \frac{g_a m^2 g_b}{s - m^2} \frac{s - \mu_M^2}{m^2 - \mu_M^2}, \\ R_{ab}^{(D)} &= \frac{m^2 - M_{CDD}^2}{m^2 - \mu_M^2} \left( \delta_{ab} - \sum_c \int_{\mu_{\text{thr}}^2}^{\infty} \frac{d\bar{s}}{\pi} \frac{m^2 - \mu_M^2}{\bar{s} - \mu_M^2} \frac{N_{ac}(\bar{s}) \rho_{cb}(\bar{s})}{\bar{s} - m^2} \right), \\ R_{ab}^{(B)} &= -\frac{\mu_M^2 - M_{CDD}^2}{(\mu_M^2 - m^2)^2} g_a m^2 g_b \\ &\quad - \sum_{c,d} \int_{\mu_{\text{thr}}^2}^{\infty} \frac{d\bar{s}}{\pi} \frac{\bar{s} - M_{CDD}^2}{\bar{s} - \mu_M^2} \frac{N_{ac}(\bar{s}) \rho_{cd}(\bar{s})}{(\bar{s} - m^2)^2} g_d m^2 g_b \\ &\quad + (m^2 - M_{CDD}^2) \sum_{c,d} \int_{\mu_{\text{thr}}^2}^{\infty} \frac{d\bar{s}}{\pi} \frac{N_{ac}(\bar{s}) \rho_{cd}(\bar{s}) U_{db}^{\text{eff}}(\bar{s})}{(\bar{s} - \mu_M^2)(\bar{s} - m^2)}. \end{aligned} \quad (14)$$

The merit of the ansatz (13, 14) lies in its specification of the CDD pole parameters,  $R^{(D)}$  and  $R^{(B)}$ , in terms of the parameters,  $g_a, m$ , characterizing a possible pole term in the generalized potential. They have to be dialed such that the effective potential  $U_{ab}^{\text{eff}}(s)$  is regular at  $s = m^2$ . The CDD pole mass parameter,  $M_{CDD}$ , is irrelevant. By construction, the scattering amplitude, which results from (11-14), does not depend on the choice of  $M_{CDD}$ .

The system (13, 14) can be solved numerically by matrix inversion techniques. Once we obtain a solution of  $N_{ab}(s)$ , we can compute  $D_{ab}(s)$  via (12), and a well defined result for the partial-wave scattering amplitude is obtained with (11).

## 4 Numerical results

Our results rely on the choice of various parameters. We use  $f = 90$  MeV in the following, where we checked that small variations around that value lead to



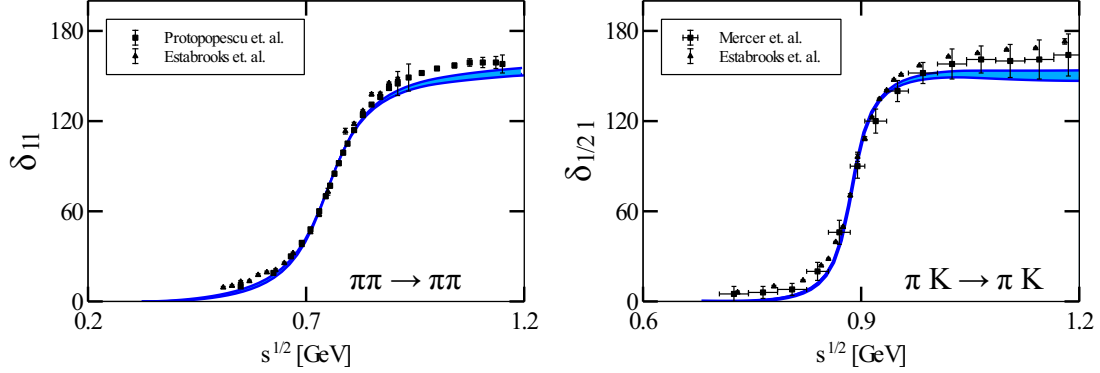


Fig. 1. p-Wave scattering phases  $\delta$  for  $\pi\pi \rightarrow \pi\pi$  with  $I = 1$  and  $\pi K \rightarrow \pi K$  with  $I = \frac{3}{2}$ . The data are taken from [34,35,36,37].

very similar results. For the cutoff parameter  $\Lambda_s$  introduced in the conformal variable (9) we use the  $\Lambda_s = 1.4$  GeV unless stated otherwise. The small effects caused by variations around that central value will be discussed. The value of  $\Lambda_s$  sets the scale from where on s-channel physics is integrated out. In our approach the generalized potential is characterized further by the number of terms considered in the conformal expansion (10). Typically a few terms only suffice to arrive at a good approximation of the generalized potential. A large number of terms would be justified if the left-hand cut structures are modeled very accurately, or a large number of counter terms are considered. If the empirical data set would be very accurate and more complete one could determine the various coefficients in (10) directly from the data set in a model independent manner. In our approach the left-hand cut structures are defined by the t- or u-channel exchange of Goldstone boson pairs. The latter imply specific correlations of the expansion coefficients.

We begin with a presentation of partial-waves with  $J = 1$ , which probe the masses and decay properties of the light vector mesons. At tree-level the vector meson masses are

$$\begin{aligned} m_\rho^2 &= m_\omega^2 = m_{1-}^2 + b_D m_\pi^2, & m_{K^*}^2 &= m_{1-}^2 + b_D m_K^2, \\ m_\phi^2 &= m_{1-}^2 + b_D (2 m_K^2 - m_\pi^2), \end{aligned} \quad (15)$$

which leads to the estimate  $m_{1-} \simeq 0.76$  GeV and  $b_D \simeq 0.95$ . The latter values reproduce the empirical vector meson masses with an uncertainty of less than 10 MeV. Within our unitarization scheme we identify the expressions of (15) with the mass parameter  $m$  in (14). The physical  $\omega$  and  $\phi$  meson masses can be extracted from the  $(I^G, S) = (0^-, 0)$  sector, which involves the single

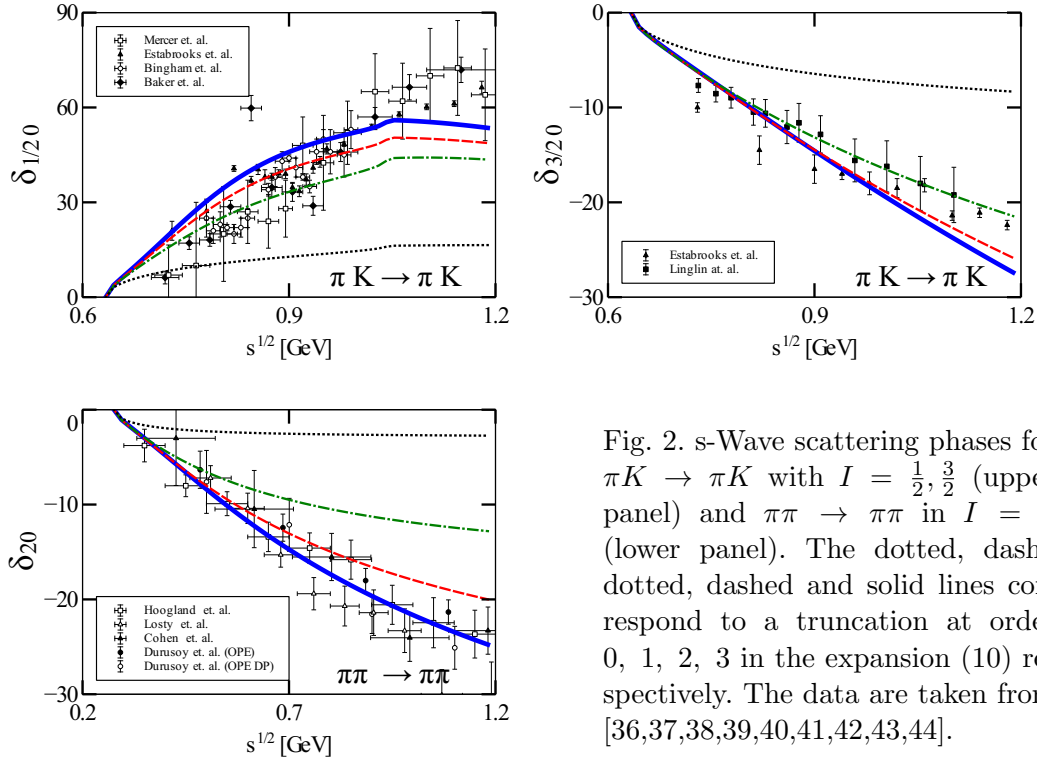


Fig. 2. s-Wave scattering phases for  $\pi K \rightarrow \pi K$  with  $I = \frac{1}{2}, \frac{3}{2}$  (upper panel) and  $\pi\pi \rightarrow \pi\pi$  in  $I = 2$  (lower panel). The dotted, dash-dotted, dashed and solid lines correspond to a truncation at order 0, 1, 2, 3 in the expansion (10) respectively. The data are taken from [36,37,38,39,40,41,42,43,44].

channel  $\bar{K}K$  only. The solution of (11-14) recovers the tree-level mass of the  $\omega$  meson identically. Since its mass is below the  $\bar{K}K$  threshold, its decay width is zero here. In contrast the  $\phi$  meson receives a small width depending on the actual value of  $h_P$ . Its mass is almost indistinguishable from its tree-level expression (15). We determine  $h_P \simeq 0.26$  as to obtain an accurate description of the  $(I, S) = (1, 0)$  and  $(I, S) = (1/2, 1)$  sectors, which are dominated by poles caused by the  $\rho$  and  $K^*$  mesons. We find that the mass parameters  $m$  in (14) needed to recover the empirical  $\pi\pi$  and  $\pi K$  phase shifts are the empirical masses of the  $\rho$  and  $K^*$  mesons. We conclude that the tree-level expressions for the vector meson masses survive the unitarization. This justifies our procedure to use physical vector meson masses in the driving expressions (5). In Fig.1 we confront our results with empirical p-wave  $\pi\pi$  and  $\pi K$  phase shifts. A good description up to about 1 GeV is achieved. The  $\rho$  and  $K^*$  mesons are clearly visible in the data and our theoretical curves. As a consistency check we computed with  $\Gamma_\phi \simeq 3.47$  MeV the width of the  $\phi$  meson. Our value is consistent with the empirical range of the partial width  $\Gamma_\phi(K\bar{K}) = 3.54 \pm 0.04$  MeV. It is amusing to observe that a universal value of  $h_P$  is able to recover the decay properties of the  $\rho$ ,  $K^*$  and  $\phi$  mesons simultaneously.

Our results are stable against variations of  $\Lambda_s$  and changing the number of terms kept in (10). A variation of  $\Lambda_s$  from 1.1 GeV to 1.6 GeV would almost not be visible in the figure and therefore we refrain from showing it. In contrast

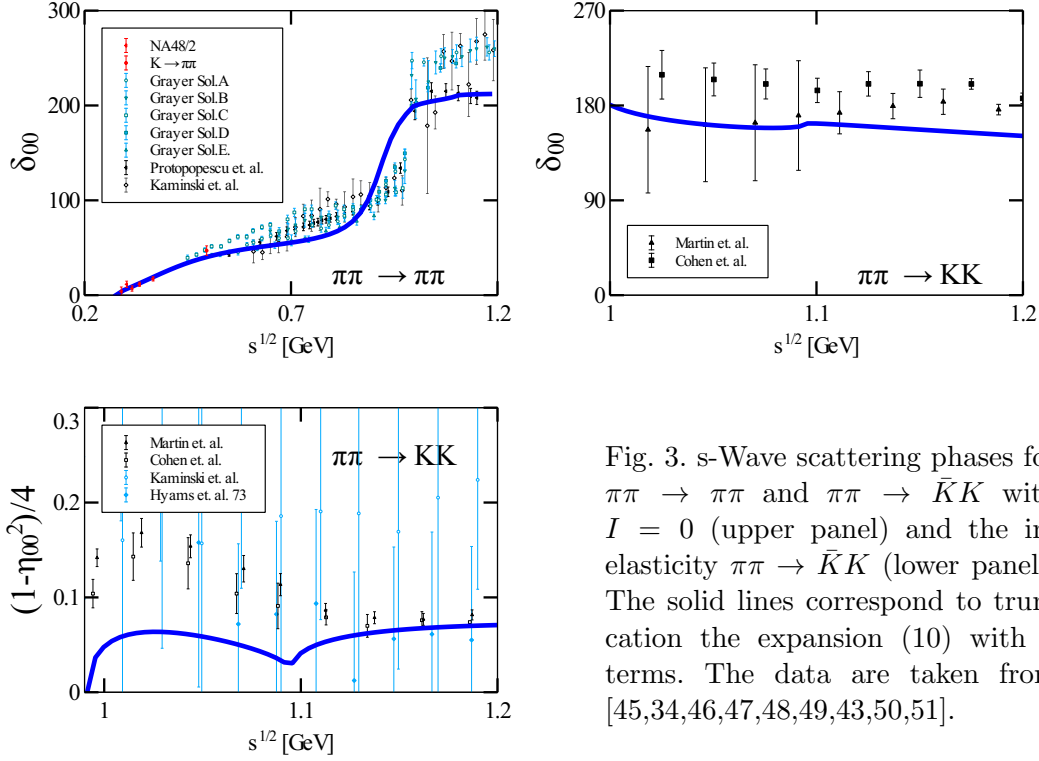


Fig. 3. s-Wave scattering phases for  $\pi\pi \rightarrow \pi\pi$  and  $\pi\pi \rightarrow \bar{K}K$  with  $I = 0$  (upper panel) and the inelasticity  $\pi\pi \rightarrow \bar{K}K$  (lower panel). The solid lines correspond to truncation the expansion (10) with 4 terms. The data are taken from [45,34,46,47,48,49,43,50,51].

decreasing the number of terms in (10) from four to one defines the bands shown in Fig.1.

We turn to a discussion of the s-waves, where we again focus on phases for which there is empirical information available. Our results for the  $\pi K$  phases are shown against empirical data in Fig.2. The figure includes also our result for the isospin two s-wave  $\pi\pi$  scattering phase. While a variation of  $\Lambda_s$  from 1.1 GeV to 1.6 GeV would barely be visible in the figure, the results are sensitive to the numbers of terms considered in (10). The figure shows the results of keeping 1 to 4 terms in (10). In all three cases there is a saturation observed, with already the 4-term approximation recovering the empirical phases within the uncertainties of the different experimental results. We conclude from this result that indeed the vector meson exchanges contributions provide a quite accurate approximation for the leading coefficients in the conformal expansion (10).

We close the presentation with a discussion of the isoscalar sector. Three different channels,  $\pi\pi$ ,  $\bar{K}K$  and  $\eta\eta$  contribute in our analysis. In Fig.3 the empirical data from  $\pi\pi$  scattering are collected and confronted against our results. The solid lines follow in the 4-term approximation. We recover the  $\pi\pi \rightarrow \pi\pi$  and  $\pi\pi \rightarrow \bar{K}K$  phases qualitatively, with some quantitative discrepancies around the  $f_0(980)$  resonance structure. The inelasticity in the  $\pi\pi \rightarrow \bar{K}K$

reaction appears to be underestimated.

Our results are in reasonable agreement with previous results from the Roy-Steiner equations [5,6,7]. With our analysis we further explored the role of explicit vector-meson degrees of freedom. Our leading order computation has basically only two free parameters  $f = 90$  MeV and  $h_P = 0.26$ . To this extend we find the agreement with the previous results based on Roy-Steiner equations [5,6,7] the very satisfactory.

## Acknowledgements

We acknowledge useful discussions with A.M. Gasparyan.

## References

- [1] E. van Beveren, T. A. Rijken, K. Metzger, C. Dullemond, G. Rupp, et al., A Low Lying Scalar Meson Nonet in a Unitarized Meson Model, *Z.Phys.* C30 (1986) 615–620.
- [2] J. D. Weinstein, N. Isgur, K anti-K Molecules, *Phys.Rev.* D41 (1990) 2236.
- [3] G. Janssen, B. C. Pearce, K. Holinde, J. Speth, On the structure of the scalar mesons  $f_0$  (975) and  $a_0$  (980), *Phys.Rev.* D52 (1995) 2690–2700.
- [4] S. M. Roy, Exact integral equation for pion pion scattering involving only physical region partial waves, *Phys.Lett.* B36 (1971) 353.
- [5] B. Ananthanarayan, G. Colangelo, J. Gasser, H. Leutwyler, Roy equation analysis of  $\pi\pi$  scattering, *Phys.Rept.* 353 (2001) 207–279.
- [6] G. Colangelo, J. Gasser, H. Leutwyler,  $\pi\pi$  scattering, *Nucl.Phys.* B603 (2001) 125–179.
- [7] P. Buettiker, S. Descotes-Genon, B. Moussallam, A new analysis of  $\pi K$  scattering from Roy and Steiner type equations, *Eur.Phys.J.* C33 (2004) 409–432.
- [8] R. Garcia-Martin, R. Kaminski, J. R. Pelaez, J. Ruiz de Elvira, F. J. Yndurain, The Pion-pion scattering amplitude. IV: Improved analysis with once subtracted Roy-like equations up to 1100 MeV, *Phys.Rev.* D83 (2011) 074004.
- [9] S. Weinberg, Phenomenological Lagrangians, *Physica* A96 (1979) 327, festschrift honoring Julian Schwinger on his 60th birthday.
- [10] J. Gasser, H. Leutwyler, Chiral Perturbation Theory to One Loop, *Annals Phys.* 158 (1984) 142.

- [11] M. Knecht, B. Moussallam, J. Stern, N. Fuchs, The Low-energy  $\pi\pi$  amplitude to one and two loops, Nucl.Phys. B457 (1995) 513–576.
- [12] J. Bijnens, G. Colangelo, G. Ecker, J. Gasser, M. E. Sainio, Elastic  $\pi\pi$  scattering to two loops, Phys.Lett. B374 (1996) 210–216.
- [13] J. Bijnens, G. Colangelo, G. Ecker, J. Gasser, M. E. Sainio, Pion pion scattering at low-energy, Nucl.Phys. B508 (1997) 263–310.
- [14] J. A. Oller, E. Oset, Chiral symmetry amplitudes in the S wave isoscalar and isovector channels and the  $\sigma$ ,  $f_0(980)$ ,  $a_0(980)$  scalar mesons, Nucl.Phys. A620 (1997) 438–456.
- [15] V. Bernard, N. Kaiser, U. G. Meissner, Chiral perturbation theory in the presence of resonances: Application to  $\pi\pi$  and  $\pi K$  scattering, Nucl.Phys. B364 (1991) 283–320.
- [16] M. Jamin, J. A. Oller, A. Pich, S wave  $K\pi$  scattering in chiral perturbation theory with resonances, Nucl.Phys. B587 (2000) 331–362.
- [17] A. Gomez Nicola, J. R. Pelaez, Meson meson scattering within one loop chiral perturbation theory and its unitarization, Phys. Rev. D65 (2002) 054009.
- [18] M. F. M. Lutz, S. Leupold, On the radiative decays of light vector and axial-vector mesons, Nucl.Phys. A813 (2008) 96–170.
- [19] G. Ecker, J. Gasser, A. Pich, E. de Rafael, The Role of Resonances in Chiral Perturbation Theory, Nucl.Phys. B321 (1989) 311.
- [20] M. F. M. Lutz, E. E. Kolomeitsev, On meson resonances and chiral symmetry, Nucl.Phys. A730 (2004) 392–416.
- [21] S. Leupold, M. F. M. Lutz, Hadronic three-body decays of light vector mesons, Eur.Phys.J. A39 (2009) 205–212.
- [22] A. Gasparyan, M. F. M. Lutz, Photon- and pion-nucleon interactions in a unitary and causal effective field theory based on the chiral Lagrangian, Nucl.Phys. A848 (2010) 126–182.
- [23] I. V. Danilkin, A. M. Gasparyan, M. F. M. Lutz, On causality, unitarity and perturbative expansions, Phys.Lett. B697 (2011) 147–152.
- [24] A. Krause, Helv. Phys. Acta 63 (1990) 3–70.
- [25] M. F. M. Lutz, E. E. Kolomeitsev, Relativistic chiral SU(3) symmetry, large N(c) sum rules and meson baryon scattering, Nucl.Phys. A700 (2002) 193–308.
- [26] M. F. M. Lutz, E. E. Kolomeitsev, Covariant meson baryon scattering with chiral and large N(c) constraints, Found.Phys. 31 (2001) 1671–1702.
- [27] M. F. M. Lutz, E. E. Kolomeitsev, C. L. Korpa, Chiral symmetry, strangeness and resonances, Prog. Theor. Phys. Suppl. 156 (2004) 51–71.
- [28] M. F. M. Lutz, E. E. Kolomeitsev, Baryon resonances from chiral coupled-channel dynamics, Nucl. Phys. A755 (2005) 29–39.

- [29] A. M. Gasparyan, M. F. M. Lutz, B. Pasquini, Compton scattering from chiral dynamics with unitarity and causality, Nucl.Phys. A866 (2011) 79–92.
- [30] G. F. Chew, S. Mandelstam, Theory of low-energy pion pion interactions, Phys.Rev. 119 (1960) 467–477.
- [31] L. Castillejo, R. H. Dalitz, F. J. Dyson, Low’s scattering equation for the charged and neutral scalar theories, Phys.Rev. 101 (1956) 453–458.
- [32] J. A. Oller, E. Oset, N/D description of two meson amplitudes and chiral symmetry, Phys.Rev. D60 (1999) 074023.
- [33] A. P. Szczepaniak, P. Guo, M. Battaglieri, R. De Vita, P-wave pi pi amplitude from dispersion relations, Phys.Rev. D82 (2010) 036006.
- [34] S. D. Protopopescu, M. Alston-Garnjost, A. Barbaro-Galtieri, S. M. Flatte, J. Friedman, et al., Phys. Rev. D7 (1973) 1279.
- [35] P. Estabrooks, A. D. Martin, pi pi Phase Shift Analysis Below the K anti-K Threshold, Nucl.Phys. B79 (1974) 301.
- [36] R. Mercer, P. Antich, A. Callahan, C.-Y. Chien, B. Cox, et al., Nucl. Phys. B32 (1971) 381.
- [37] P. Estabrooks, R. K. Carnegie, A. D. Martin, W. M. Dunwoodie, T. A. Lasinski, et al., Nucl. Phys. B133 (1978) 490.
- [38] H. H. Bingham, W. M. Dunwoodie, D. Drijard, D. Linglin, Y. Goldschmidt-Clermont, et al., Nucl. Phys. B41 (1972) 1–34.
- [39] S. L. Baker, S. Banerjee, J. R. Campbell, G. Hall, A. K. M. A. Islam, et al., Nucl. Phys. B99 (1975) 211.
- [40] D. Linglin, B. Chaurand, B. Drevillon, G. Labrosse, R. Lestienne, et al., Nucl. Phys. B57 (1973) 64–76.
- [41] W. Hoogland, S. Peters, G. Grayer, B. Hyams, P. Weilhammer, et al., Measurement and Analysis of the pi+ pi+ System Produced at Small Momentum Transfer in the Reaction  $\pi^+p \rightarrow \pi^+\pi^+n$  at 12.5-GeV, Nucl.Phys. B126 (1977) 109.
- [42] M. J. Losty, V. Chaloupka, A. Ferrando, L. Montanet, E. Paul, et al., A Study of  $\pi^-\pi^-$  scattering from  $\pi^-p$  interactions at 3.93-GeV/c, Nucl. Phys. B69 (1974) 185–204.
- [43] D. H. Cohen, D. S. Ayres, R. Diebold, S. L. Kramer, A. J. Pawlicki, et al., Phys. Rev. D22 (1980) 2595.
- [44] N. B. Durusoy, M. Baubillier, R. George, M. Goldberg, A. M. Touchard, et al., Phys. Lett. B45 (1973) 517–520.
- [45] G. Grayer, B. Hyams, C. Jones, P. Schlein, P. Weilhammer, et al., Nucl. Phys. B75 (1974) 189.

- [46] R. Kaminski, L. Lesniak, K. Rybicki, Separation of S wave pseudoscalar and pseudovector amplitudes in  $\pi^- p$  (polarized)  $\rightarrow \pi^+ \pi^- n$  reaction on polarized target, Z. Phys. C74 (1997) 79–91.
- [47] J. R. Batley, A. J. Culling, G. Kalmus, C. Lazzeroni, D. J. Munday, et al., Eur. Phys. J. C54 (2008) 411.
- [48] V. Cirigliano, G. Ecker, A. Pich, Reanalysis of pion pion phase shifts from  $K \rightarrow \pi\pi$  decays, Phys.Lett. B679 (2009) 445–448.
- [49] A. D. Martin, E. N. Ozmütlu, Analyses of  $K\bar{K}$  production and scalar mesons, Nucl. Phys. B158 (1979) 520.
- [50] R. Kaminski, L. Lesniak, K. Rybicki, A Joint analysis of the S wave in the  $\pi^+\pi^-$  and  $\pi^0\pi^0$  data, Eur. Phys. J. direct C4 (2002) 4.
- [51] B. Hyams, C. Jones, P. Weilhammer, W. Blum, H. Dietl, et al.,  $\pi\pi$  Phase Shift Analysis from 600-MeV to 1900-MeV, Nucl. Phys. B64 (1973) 134–162.